Nucleation theory near the classical spinodal

Chris Unger and W. Klein
Center for Polymer Studies and Department of Physics, Boston University, Boston, Massachusetts 02215
(Received 5 July 1983; revised manuscript received 18 November 1983)

We present a field-theoretic description of metastability and nucleation for arbitrary range interaction models near the limit of metastability, i.e., spinodal. We find that as the spinodal is approached, the size of the nucleating droplet diverges in all dimensions. The upper critical dimension is found to be six. For $d<6$, as the spinodal is approached the nucleating droplets become ramified and their free-energy cost goes to zero; thus the system nucleates before reaching the spinodal. The free-energy cost increases rapidly as the range of the interaction, R, is increased, so that even for $d<6$ the spinodal can be approached as close as desired by increasing R. The internal structure of the ramified droplets in all dimensions is mapped onto that of a percolation cluster. The lifetime, including both the free-energy cost of the nucleating droplet and a dynamic prefactor, diverges in all dimensions; this is due to "critical" slowing down as the spinodal is approached. For $d>6$, the free-energy cost of the ramified droplets diverges as the spinodal is approached; more compact droplets must also be considered. A crossover where the upper critical dimension changes continuously from 6, for spinodal behavior, to 4, for critical-point behavior, is found for the model; this crossover is hypothesized to be absent or unobservable for more realistic models. The initial growth of the droplet is found to take place through compactification rather than through radial accretion as occurs in nucleation near the coexistence curve.

I. INTRODUCTION

The question of how to treat metastable, rather than stable, states within thermodynamics has long been a challenge.[1-5] van der Waals's original mean-field theory for the equation of state of gases and liquids predicted both metastable and unstable states and did not predict phase coexistence. Maxwell's construction gives an *ad hoc* way of setting phase coexistence into the theory and leaves the meaning of the metastable states undetermined. Lebowitz and Penrose[4] have shown that as the interaction between particles becomes very long range and weak, the equilibrium equation of state is van der Waals's equation (i.e., mean field) with Maxwell's construction, with no metastable or unstable states.

Penrose and Lebowitz[6] have shown that in the thermodynamic and infinite-range interaction limits the mean-field theory for the metastable state also becomes exact and the nucleation rate goes to 0. However, they were unable to make any calculations for large but finite R in the thermodynamic limit. Monte Carlo simulations have been done on Ising models with long-range interactions using the equivalent neighbor model;[7] in this model each spin has a uniform ferromagnetic coupling with all other spins within a block size of R. It has been found that as R is increased the metastable state remains well defined for deeper quenches.[8] These simulations for three dimensions indicate that the mean-field theories for the metastable state, although not correct for small R, become increasingly accurate with larger interaction range.[8-10]

An approach which is complementary to mean-field theories is the classical droplet model of nucleation.[11,12] This model gives a good description of the decay of the metastable states in various systems, from Ising models to fluids. This model, however, assumes that the nucleating droplet is a compact fluctuation of the stable phase (i.e., its fractal dimension d_f is equal to d, the dimension of space; see below). While this assumption may be appropriate near the coexistence curve, where the metastable and stable states are degenerate in free energy, for deep quenches near the spinodal, any compact droplet is past the nucleating stage and well into the growth phase. The nucleating droplet is expected to be of small amplitude and ramified ($d_f<d$).[13]

There has recently been an attempt to generalize the droplet model by including nonclassical exponents in the theory.[14] As might be expected, this model gives reasonable results for scaling and the ramified droplet profiles. The theory assumes the existence of spinodal singularities, and hence cannot predict whether the spinodal is sharp and approachable, or whether the spinodal is unreachable and only a pseudospinodal.

In a recent communication,[15] we developed a field-theoretic description for metastability and nucleation for arbitrary range interaction models near the spinodal. This extends the work of Langer[5] and Cahn and Hilliard.[3] Langer[5] studied nucleation near the coexistence curve for systems with nonconserved order parameter in three dimensions; Cahn and Hilliard[3] studied nucleation for systems with conserved order parameter in three dimensions both near the coexistence curve and near the spinodal region. We study systems with a long-range interaction and nonconserved order parameter near the spinodal region for arbitrary dimension. The spinodal region becomes sharper as the range of the interaction increases, and in the limit of infinite-range interaction becomes a spinodal line described by a mean-field theory. In contrast, cluster dynamical theories of metastability for short-range poten-

tials show a smooth crossover between nucleation and spinodal decomposition.[16] We found that the nucleating droplet is isomorphic to a percolation cluster. We also found that the droplet has a diverging radius and a vanishing density difference from the background for all dimensions, and that the free-energy cost of ramified droplets vanishes near the spinodal for $d<6$, consistent with Cahn and Hilliard's[3] results for $d=3$. This result should be compared to those of Billotet and Binder,[17] who worked with short-range potentials in arbitrary dimension and found a finite, nonvanishing free-energy barrier to nucleation throughout an extended spinodal region.

For $d<6$ and fixed value of the range of the potential, both the lifetime of the metastable state and the sharpness with which the state is defined decline as the "spinodal" is approached;[15] only pseudospinodals,[18,19] or apparent singularities, are predicted. This is consistent with the work of Chu, Schoenes, and Fisher,[18] who showed that spinodal exponents could be derived from an extrapolation of measurements of the stable state, and with the work of Speedy and Angell[19] who measured thermodynamic quantities in supercooled water. Both experimental systems showed no signs of a reachable physical singularity; however, one could find well-defined spinodal exponents by extrapolating the data. It has been conjectured[13] that the spinodal exponents derived from such an expansion are well defined, but that the location of the extrapolated spinodal temperature is not. This conjecture is consistent with renormalization-group calculations and Monte Carlo simulations of the coarsed-grained free energy,[20,21] and with dynamical theories of nucleation.[22,23] We found, in agreement with previous work, that the location of the spinodal depends on the coefficients appearing in the free energy, but that the spinodal exponents depend only on the form of the free energy.

In this paper we extend our previous results and also treat the initial growth of the nucleating droplet. The remainder of this paper is structured as follows. In Sec. II we show that as the range of the interaction increases, the metastable state becomes more sharply defined, and calculate the nucleating droplet's profile, free-energy cost, and initial growth pattern. In Sec. III the internal structure of the nucleating droplet is shown to be isomorphic to that of a percolation cluster. In Sec. IV we compute the lifetime of the metastable state near the spinodal. Section V compares our results to previous work.

II. THE NUCLEATING DROPLET PROFILE AND FREE-ENERGY COST

In this paper we work with the partition function derived from a ψ^4-field-theoretic Hamiltonian

$$Z=\int d\psi e^{-H(\psi)}, \tag{2.1a}$$

$$H(\psi)=\int d^dr\left[\frac{1}{2}\frac{\beta}{\beta_0}R^2(\nabla\psi)^2-\frac{1}{2}\left[\frac{\beta}{\beta_0}-1\right]\psi^2(r)+\beta a\psi^4(r)+\beta h\psi(r)\right], \tag{2.1b}$$

where R can be identified with the range of the interaction,[5] $\beta=1/kT$ where T is the temperature, β_0 is the value of β at the critical point, h is the magnetic field, and a is a positive constant. This Hamiltonian can be shown to be a model for Ising models near their critical point.

Following Langer,[5] we rescale variables $\sigma=R(\beta/\beta_0)^{1/2}\psi$ and introduce the reduced parameters

$$\epsilon=\frac{1}{2R^2}\left[1-\frac{\beta_0}{\beta}\right], \tag{2.2a}$$

$$\alpha=\frac{\beta_0 a}{\beta R^4}, \tag{2.2b}$$

and

$$\lambda=(\beta\beta_0)^{1/2}h/R. \tag{2.2c}$$

The free energy becomes

$$F(\sigma)=\int d^dr[\tfrac{1}{2}(\nabla\sigma)^2-\epsilon\sigma^2+\alpha\sigma^4+\lambda\sigma]. \tag{2.3}$$

For much of what we do later, a further rescaling is useful:

$$s=\sqrt{\epsilon}r=\frac{r}{R}\left[\frac{1-\beta/\beta_0}{2}\right]^{1/2},$$

and (2.4)

$$\sigma(r)=(\epsilon/2\alpha)^{1/2}u(s).$$

Equation (2.3) can be rewritten as

$$F(u)=\frac{\epsilon^{2-d/2}}{2\alpha}\int d^ds\left[\tfrac{1}{2}(\nabla_s u)^2+\tfrac{1}{2}u^4-u^2+\frac{4}{3\sqrt{3}}\tilde{\lambda}u\right], \tag{2.5}$$

with $\tilde{\lambda}=\lambda/\lambda_s$ and $\lambda_s=(8\epsilon^3/27\alpha)^{1/2}$. The meaning of λ_s will be made clear shortly.

For large values of $\epsilon^{2-d/2}/2\alpha$, the Hamiltonian has deep valleys as a function of $u(r)$ and the probability of finding a state $P(u)=e^{-H(u)}/Z$ is sharply peaked around $u_{\min}$, with the value of u at the minimum of $H(u)$. Thus, we have a set of well-defined states, and we can regard $H(u_{\min})$ equivalently as an energy or as a free energy of a state.

The integrand in Eq. (2.5) is an effective free-energy density. The stable and metastable states are uniform to minimize the gradient-squared term in the free energy and lie at the local minima of the quartic polynomial in $F(u)$. For $\epsilon>0$, i.e., for $T>T_c$, the u^2 term enters with a positive sign and there is exactly one minimum, the global minimum, as shown in Fig. 1 (a). There are no coexisting and no metastable states. For $T<T_c$ and small $\tilde{\lambda}$, the local free energy increases without bound for large u and has two minima and one maximum, as shown in Fig. 1(b). While the uniform state with the lower free energy is absolutely stable, the other minimum is metastable and the system can become trapped near that minimum. On the other hand, if $\tilde{\lambda}$ is sufficiently large the free energy has just one local minimum again, as shown in Fig. 1(d). Even though $T<T_c$, the metastable state has disappeared. The value $\lambda_s(T)$ is that value of λ for which the shallower well disappears. The location of the well as it disappears is $u_{\rm sp}=1/\sqrt{3}$.

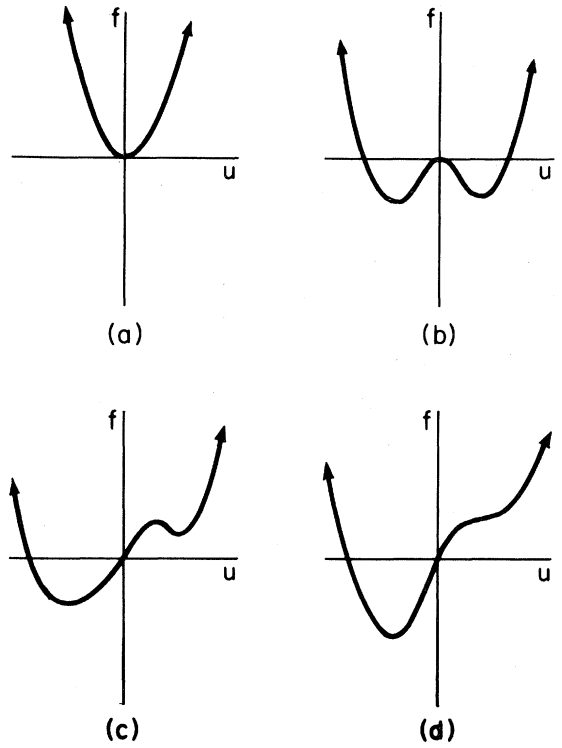

FIG. 1. Schematic plot of "ψ^4" mean-field free-energy density f for various temperatures and magnetic fields. (a) is for $T>T_c$, (b) is for $T<T_c$ and $h=0$, (c) is for $T<T_c$ and $0<h<h_s$, and (d) is for $T<T_c$ and $h=h_s$.

For λ near λ_s, the well is shallow and fluctations, which do not nucleate the system, will be confined to small displacements around u_{sp}. The free energy is then effectively the pure cubic pictured in Fig. 2. Rewriting F in terms of the variable $v=u-1/\sqrt{3}$, we find

$$F(v)=\frac{\epsilon^{2-d/2}}{2\alpha}\int d^dS\left[\tfrac{1}{2}(\nabla_s v)^2+\tfrac{1}{2}v^4+\frac{2}{\sqrt{3}}v^3-\frac{4}{3\sqrt{3}}\Delta\tilde{\lambda}v\right], \tag{2.6}$$

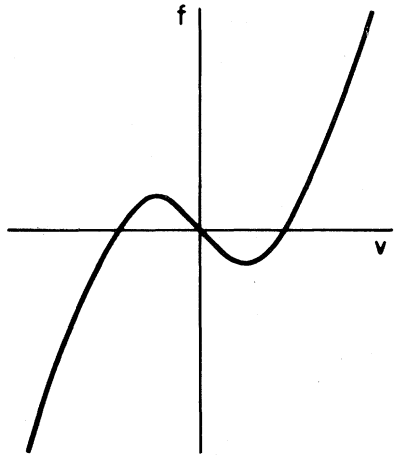

FIG. 2. Free-energy density f near the metastable minimum for h just smaller than h_s.

where $\Delta\tilde{\lambda}=1-\lambda/\lambda_s$. We can evaluate the partition function in the limit $\epsilon^{2-d/2}/2\alpha\to\infty$ by the method of steepest descent. This evaluation is equivalent to replacing $H(u)$ by a quadratic approximation near its stationary points and performing the resulting Gaussian integrals, while ignoring the value of $e^{-H(u)}$ everywhere else. The magnitude of the partition function for the metastable state can be found by expanding around the shallower of the two minima of the local free energy. The approximation of calculating the partition function by including the contribution from the smaller maxima while ignoring the larger maxima, is the analytic continuation of the partition function in the complex λ plane.[5] The partition function becomes complex when it is analytically continued into the metastable region, and the lifetime of the metastable state is related to its imaginary part.[5] The imaginary part can be found to be of lowest order by expanding around the saddle-point function separating the stable and metastable minima. Thus, we see that the lowest-order approximations to the real and imaginary parts of Z are given by the metastable minima and the saddle point, respectively.

We now apply quasiequilibrium thermodynamic arguments[2,3,5] to the metastable state. We can do this if the metastable state lasts sufficiently long to be observed experimentally; our approximations are self-consistent only as long as the predicted lifetime of the metastable state remains large. Within this quasiequilibrium picture, the nucleating droplet lies on the boundary between those fluctuations which lower their free energy by growing and those that lower their free energy by shrinking. Thus, the nucleating droplet is a stationary point of the free-energy functional, and its density profile satisfies the Euler-Lagrange equation[5]

$$\frac{\delta F(v)}{\delta v(s)}=-\nabla_s^2 v+2v^3+\frac{6}{\sqrt{3}}v^2-\frac{4}{3\sqrt{3}}\Delta\tilde{\lambda}=0\ . \tag{2.7}$$

Making the assumption that the profile of the nucleating droplet depends only on the radius, Eq. (2.7) reduces to

$$-\frac{d^2v}{ds^2}-\frac{d-1}{s}\frac{dv}{ds}+2v^3+\frac{6}{\sqrt{3}}v^2-\frac{4}{3\sqrt{3}}\Delta\tilde{\lambda}=0\ . \tag{2.8}$$

If we were dealing with an interface whose thickness were small compared to its radius of curvature, we could neglect the $[(d-1)/s]dv/ds$ term. One can argue that this is justified near $h=0$,[5] where the stable and metastable states are nearly degenerate, but it is not justified here. Nevertheless, since $[(d-1)/s]dv/ds$ scales just as d^2v/ds^2, and neglecting that it does not change the order of the equation, ignoring the first derivative term will only change the shape of the profile. Our main conclusions will be unaltered by this approximation, assuming that Eq. (2.8) has a bounded solution. In the Appendix we show that a bounded solution to Eq. (2.8) exists, for sufficiently small $\Delta\tilde{\lambda}$ [a numerical solution to Eq. (2.8) for small $\Delta\tilde{\lambda}$ is shown below in Fig. 5]. If we neglect the first derivative, Eq. (2.8) becomes

$$-\frac{d^2v}{ds^2}+2v^3+\frac{6}{\sqrt{3}}v^2-\frac{4}{3\sqrt{3}}\Delta\tilde{\lambda}=0\ . \tag{2.9}$$

Equation (2.9) can be solved exactly. It is the equation of motion for a particle of unit mass having displacement $v(s)$ moving in a potential

$$V(v)=-\tfrac{1}{2}v^4-\frac{2}{\sqrt{3}}v^3+\frac{4}{3\sqrt{3}}\Delta\tilde{\lambda}v\ ,$$

with s representing time. $V(v)$ is pictured in Fig. 3(a). Since Eq. (2.9) contains no damping term, the solution $v(s)$ will either go off to infinity or oscillate forever inside the well. In either case the free-energy cost of the fluctuation is proportional to the volume of the system. Only if the energy of the particle is exactly equal to the height of the smaller peak can the particle make one bounded fluctuation away from its background value. That fluctuation is a nucleating droplet. One can, of course, superimpose well separated, i.e., independent, droplets to obtain stationary states of the free energy containing more than one nucleating droplet.

Near the spinodal line, $\Delta\tilde{\lambda}\to 0$, nucleating droplets must have amplitudes similar to the width of the shallow well, which is going to 0 as $(\Delta\tilde{\lambda})^{1/2}$. Droplets which have larger amplitudes have already nucleated the system and are growing. Since v is small, we can neglect the v^4 with respect to the v^3 term in the free energy and in Eq. (2.9), and find that the solution for the profile of the nucleating droplet to be

$$\bar{v}=\frac{\sqrt{2\Delta\tilde{\lambda}}}{3}\{1-3\,\mathrm{sech}^2[(\tfrac{2}{3}\Delta\tilde{\lambda})^{1/4}s]\}\ . \tag{2.10}$$

We note that for $h\neq 0$ there is a well-defined length scale for nucleation $s_c\sim(\Delta\tilde{\lambda})^{-1/4}$; in contrast, near $h=0$,[5] the two states are degenerate and there is no well-defined length scale. Near $h=0$ only the interface profile can be obtained from the Euler-Lagrange Eq. (2.8) without resort to numerical integration; to derive a critical radius an effective droplet model is used.[5] We will find below that if one tries to define a "nonentropic" droplet model for quenches near the spinodal, the critical radius scales out of the problem.

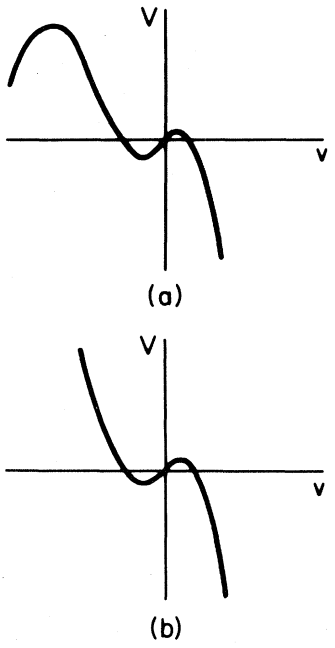

FIG. 3. Sketch of the effective potential for particle motion in Eq. (2.9). (a) is before the v^4 term is neglected, while (b) is without the quartic term. For particles moving in the well, the two potentials are nearly identical.

Inserting the original constants into the expression for s_c, or equivalently r_c, we obtain $r_c\sim R(h_s-h)^{-1/4}\propto\xi$, where ξ is the correlation length. We see that, for all dimensions, the length scale for nucleation diverges as the magnetic field approaches its spinodal value. For three dimenions, this has been noted before by Cahn and Hilliard.[3]

Inserting Eq. (2.10) in Eq. (2.6), we can now calculate the free-energy cost of the nucleating droplet near the spinodal as

$$\Delta F=F(v)-F(v_{ms})$$
$$=\frac{\epsilon^{2-d/2}}{2\alpha}(\Delta\tilde{\lambda})^{3/2-d/4}\int d^dz[f(z)+O((\Delta\tilde{\lambda})^{1/2})]\ , \tag{2.11}$$

where f is an integrable function of magnitude unity. Thus, in terms of R and h, $\Delta F\sim R^d(h_s-h)^{(3/2-d/4)}$. We see that for fixed R, the free-energy cost of a ramified nucleating droplet decreases as h approaches its spinodal value for $d<6$, while the cost increases for $d>6$. Thus, we expect to find when calculating lifetimes that for $d>6$ the system remains in the metastable state as $h\to h_s$ and our approximations are consistent; for $d<6$, however, the barrier to nucleation decreases as we approach the apparent spinodal, and thermal fluctuations will prevent the system from actually reaching the spinodal. The upper critical dimension, above which a mean-field approximation is self-consistent, is thus $d_c=6$, in agreement with earlier work.[13,24] Actually, there are nucleating paths with finite free-energy cost both above and below six dimensions.[25] Below six dimensions, the ramified droplets are important since their free-energy cost is going to 0 at the spinodal; above six dimensions, the ramified droplets have a diverging free-energy cost and the more compact droplets nucleate the system. The free-energy cost is always proportional to the volume of interaction R^d, and increasing R will allow quenches closer to the spinodal magnetic field before ΔF becomes of the order of kT.

For dimensions smaller than the upper critical dimension, the free-energy cost of the nucleating droplet becomes smaller as h approaches the value h_s. As the free-energy cost approaches the average thermal fluctuation energy kT, the critical droplets become easy to excite. The metastable state becomes less sharply defined as its average lifetime decreases, and the nucleating droplets lose their identity as they become more numerous and start interacting. One observes the beginnings of a spinodal-like singularity,[8] as in high dimensions, but this potential singularity is masked by thermal fluctuations and nucleation, leaving only a pseudospinodal.[1,18,19,26]

Speedy and Angell[19] have observed pseudospinodals in supercooled H_2O and D_2O. The measured thermodynamic quantities appear to be diverging if extrapolated to lower temperatures, but the system nucleates before it can

be cooled to very close to the supposed singular temperature. However, the exponents found from the extrapolation are reproducible.

In deriving $d_c=6$, we have assumed that the temperature dependence of the coefficient in front of the integral in Eq. (2.11) can be neglected. This assumption is valid if the quench is done away from the critical point; such a quench might follow path a in Fig. 4. Along this path $\Delta\tilde{\lambda}\to 0$, while ϵ and α approach constants. Since the coexistence curve and the spinodal line become tangent at the critical point, there are quenches that display critical behavior and spinodal behavior at the same time; quenches of this type have been studied both experimentally[27–30] and theoretically.[31–33] A quench along a path similar to b in Fig. 4 has $\epsilon\to 0$, and perhaps has $\Delta\tilde{\lambda}\to 0$. Since $h_s(T)\to 0$ at the same time as $h\to h_s$ along these paths, $\Delta\tilde{\lambda}$ can go to a constant, or it can approach 0 at any rate (relative to how fast ϵ is going to 0) we choose. Binder has shown,[33] using a Ginzburg criterion, that the upper critical dimension is 4 if the quench approaches the critical point much faster than it becomes asymptotic to the spinodal line. To study the general quench path let us assume that $\Delta\tilde{\lambda}\to 0$ as $\Delta\tilde{\lambda}\sim\epsilon^{\delta}$, where $0\le\delta\le\infty$. Then the upper critical dimension, where the free-energy cost in Eq. (2.11) neither diverges nor goes to 0, becomes

$$d_c=\frac{8+6\delta}{2+\delta}\ . \tag{2.12}$$

For $\delta=0$ we recover Binder's result $d_c=4$, while for $\delta\to\infty$ we recover the above result that $d_c=6$ away from the critical point. Depending on exactly how quickly the quench path becomes asymptotic to the spinodal line, the upper critical dimension for the path varies continuously from 4 to 6.

It is instructive to try to obtain the free-energy cost of the nucleating droplet from a droplet model, with a surface and a volume term. Following Langer,[5] we use the fact that the nucleating droplet, of radius s_c, obeys the Euler-Lagrange equation to write

$$\int(\nabla_s\bar{v})^2 d^d s=-\int\bar{v}(\nabla_s^2\bar{v})$$
$$=-\int\bar{v}\left[2\bar{v}^3+\frac{6}{\sqrt{3}}\bar{v}^2-\frac{4}{3\sqrt{3}}\Delta\tilde{\lambda}\bar{v}\right]d^d s\ . \tag{2.13}$$

With the use of this result, the equation for the free-energy cost becomes

$$\Delta F=\frac{\epsilon^{2-d/2}}{2\alpha}\int d^d s\left[-\frac{\bar{v}^4}{2}-\frac{1}{\sqrt{3}}\bar{v}^3-\frac{2\Delta\tilde{\lambda}}{3\sqrt{3}}\bar{v}\right]. \tag{2.14}$$

A bulk contribution to the free-energy cost is obtained by evaluating the integrand of Eq. (2.14) at $v(0)$ and multiplying this term by $\frac{4}{3}\pi s_c^3$. Langer[5] argued that only the v^4 term contributes to the surface energy; this term can be integrated, multiplied by ds (no s^2), and the result multiplied by $4\pi s_c^2$. While this method of deriving a droplet model is valid near $h=0$, it fails near the spinodal; there is no distinction between bulk and surface terms when the droplet radius and interface length scales are not independent. This statement is consistent with computer simulations on the three-dimensional Ising model.[9]

If we were to attempt to formulate a purely energetic droplet model in the neighborhood of $h=h_s$, following Langer,[5] perhaps by using $v(s)=f(s/s_c)$ in Eq. (2.10), we would find that the critical radius simply scales out as it did in Eq. (2.11). With the use of Eq. (2.8) to relate the scale of s to the magnitude of f, one finds for three dimensions that $\Delta F=CR^3(\Delta\tilde{\lambda})^{-3/4}=Cr_c^3$ with no contribution proportional to r_c^2. The interfacial energy is proportional to the volume of the droplet, as is the bulk energy. Thus, we expect the droplets to be fractals, having surface proportional to volume. Thus, a droplet model for large magnetic fields must include the entropy.[9] We will show later that the droplets can be mapped onto percolation clusters, which are fractals. This simple scaling is due to the neglect of the v^4 term; away from the spinodal line, where this term is not negligible, the coefficient of this term remains as a nontrivial parameter even after scaling the radius and the droplet amplitude.

Having found the critical profile, we look at small perturbations around the nucleating droplets. We write $v(s)=\bar{v}(s)+\nu(s)$ and expand the free energy to second order in the perturbation ν:

$$F(v)=F(\bar{v})+F''(\nu)\ , \tag{2.15}$$

where

$$F''(\nu)=\frac{\epsilon^{2-d/2}}{2\alpha}\int d^d s\left[\tfrac{1}{2}(\nabla_s\nu)^2+\frac{6}{\sqrt{3}}\bar{v}\nu^2+3\bar{v}^2\nu^2\right]. \tag{2.16}$$

We wish to find the directions $\nu(s)$ in which the free-energy functional decreases; those directions are the modes by which the nucleating droplet initially grows or decays. We can diagonalize the quadratic form by solving the Schrödinger equation

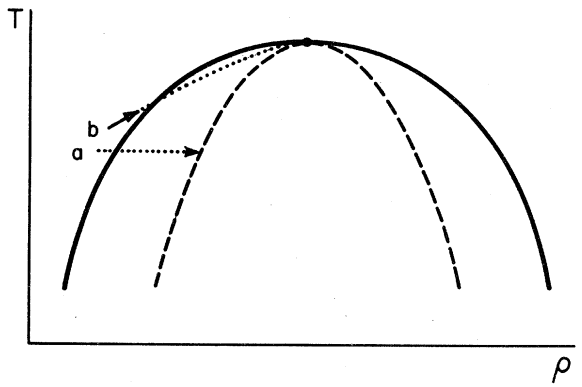

FIG. 4. Phase diagram for first-order phase transition showing a phase-coexistence curve (solid line), and the classical spinodal line (dashed line). Quenches along path a approach the spinodal while staying away from the critical point, thus, $\Delta\tilde{\lambda}\to 0$ while $\epsilon\to C$. Quenches along path b approach both the spinodal and the critical point; along these paths $\epsilon\to 0$ and $h\to h_s$ but $\Delta\tilde{\lambda}=(h_s-h)/h_s$ is not fixed by the diagram. Depending on how the path becomes asymptotic to the classical spinodal line one observes either critical behavior or spinodal behavior.

$$-\tfrac{1}{2}\nabla_s^2 v+\frac{6}{\sqrt{3}}\bar{v}v=\omega v\ , \tag{2.17}$$

or

$$\{-\tfrac{1}{2}\nabla_s^2+2(\tfrac{2}{3}\Delta\tilde{\lambda})^{1/2}-6(\tfrac{2}{3}\Delta\tilde{\lambda})^{1/2}\mathrm{sech}^2[(\tfrac{2}{3}\Delta\tilde{\lambda})^{1/4}s]\}v(s)$$
$$=\omega v(s)\ . \tag{2.18}$$

Since we use as our droplet the solution to Eq. (2.9) with the $[(d-1)/s]dv/ds$ term omitted, we wrote down Eq. (2.17) only after omitting the first derivative term. The only solution to Eq. (2.18) with a negative eigenvalue is found to be:

$$v_1(s)\propto \mathrm{sech}^3[(\tfrac{2}{3}\Delta\tilde{\lambda})^{1/4}s]\ , \tag{2.19a}$$

with

$$\omega_1=-\tfrac{5}{2}(\tfrac{2}{3}\Delta\tilde{\lambda})^{1/2}\ . \tag{2.19b}$$

From Eq. (2.15), the mode proportional to this solution is the only way for the droplet to grow and lower its free energy. As $\Delta\tilde{\lambda}\to 0$, the curvature of the free energy, which is proportional to the eigenvalue in Eq. (2.19b), goes to 0. Thus the forces driving the dynamics in this approximation are going to 0. This slowing down of the dynamics near the spinodal may be related to the "critical" slowing down suggested by Binder[26] near the spinodal.

The radius of the droplet and the radius of the initial growth mode scale with $\Delta\tilde{\lambda}$ in the same way. The initial growth mode is centered on the nucleating droplet and the radius at which the concentration has dropped to half maximum is smaller for the fluctuation than for the droplet. Consequently, the droplet grows initially by increasing its concentration at the center, while the radius of the droplet decreases. This prediction is consistent with computer simulations.[10]

Any droplet solution to Eq. (2.8) implies that there are d translational modes of that droplet which do not change the free energy. This is intuitively obvious; it is also implicit in Eq. (2.8).[5] If we apply the operator $\vec{n}\cdot\vec{\nabla}_s$ to Eq. (2.8) and set $v=\bar{v}$, we obtain

$$\left[-\nabla_s^2+6\bar{v}^2+\frac{12}{\sqrt{3}}\bar{v}\right]\vec{n}\cdot(\vec{\nabla}_s\bar{v})=0\ . \tag{2.20}$$

We dropped the $6\bar{v}^2$ term in deriving Eq. (2.17) because we are near the spinodal and $\bar{v}$ is small. If we neglect it in Eq. (2.20) we obtain, upon comparing Eq. (2.20) with Eq. (2.7), that the d infinitesimal translational modes $v_m(s)=\vec{n}_m\cdot\vec{\nabla}_s\bar{v}(s)$, with $\{\vec{n}\}$ any orthonormal basis for $\mathscr{R}^d$, are solutions to Eq. (2.7) with 0 eigenvalues. Thus, as long as $\vec{n}_m\cdot\vec{\nabla}_s\bar{v}$ is not 0, Eq. (2.7) has d solutions that are translational modes of v, and which do not change the free energy.

In order to ensure that including the first derivative term in Eq. (2.8) does not change the above results qualitatively, we solved the equation numerically for the nucleating droplet's profile in three dimensions. We then used the correct result for the nucleating droplet as a potential in Eq. (2.17) for the perturbation around the droplet. We display the results in Fig. 5. Cahn and Hilliard[3] derived an equation for the nucleating droplet profile in three dimenisons, which is equivalent to ours up to the constants. The constants cannot be compared since Cahn and Hilliard take the concentration in a fluid to be the independent variable, while we take the magnetic field in a magnetic model to be the independent variable. They solved the equation on an analog computer; their solution for the droplet profile is qualitatively similar to our profile distribution. They did not treat the fluctuation around the nucleating droplet.

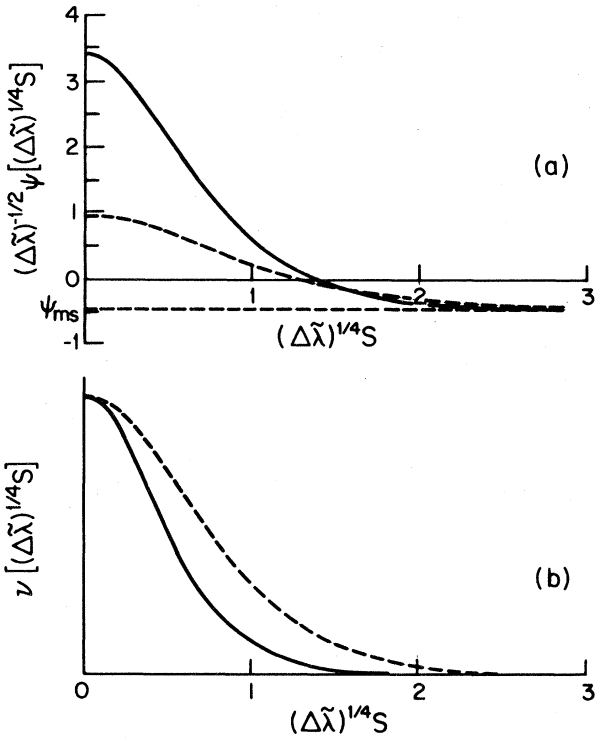

FIG. 5. Profile of the nucleating droplet and of the initial unstable mode. The droplet profile is plotted in (a) while the initial unstable mode is shown in (b). In both cases the dotted line is the analytical solution ignoring the first derivative while the solid curve is the numerical solution. The overall scale in (b) is arbitrary.

Although the profiles change slightly when the first derivative term is included in the equation, the numerical solutions scale the same way that the approximate closed-form solutions do. In both cases the fluctuation around the nucleating droplet has a smaller radius than the droplet itself, leading to an initial decrease in the mean-square radius as the droplet grows. This is consistent with the computer experiments of Heermann and Klein[10] and implies an initial compactification in the growth phase.

III. CONNECTIONS TO PERCOLATION

While we have found the average concentration of the nucleating droplet as a function of radius, we cannot make detailed predictions about the droplet's internal structure based on the coarse-grained equations above. Instead, we study the droplet structure by mapping the Hamiltonian of Eq. (2.1b) onto one for a percolation model and study the percolation clusters. A similar technique was used to describe Ising critical clusters.[34,35]

The percolation model we treat is the correlated site random-bond Ising model in d dimensions.[35] Sites are considered occupied if the spin at that site is down; the usual nearest-neighbor Ising interaction leads to correlations among sites. Bonds between adjacent sites are occupied with probability p_b. A cluster is a set of occupied sites connected to each other by occupied bonds. If $p_b=1$, any two occupied nearest-neighbor sites belong to the same cluster; as we decrease p_b the clusters become smaller and more ramified, until for $p_b=0$, all the clusters are single sites.

The connectivity properties of this model can be shown to be given by the $s\to 1$ limit of the dilute s-state Potts model[34,35] with the Hamiltonian

$$-\beta H=J\sum_{\langle ij\rangle}(s\delta_{\sigma_i,\sigma_j}-1)n_in_j-K\sum_{\langle ij\rangle}n_in_j -\Delta\sum_i n_i+H\sum_i(s\delta_{\sigma_i,1}-1)n_i\ , \tag{3.1}$$

where n_i can have the values 0 or 1, $\delta_{\sigma_i,\sigma_j}$ is the Kronecker δ function, Δ is the chemical potential which is a function of K and h, h is the Ising field, and H is the Potts field. Coniglio and Lubensky[35] mapped this problem onto a field theory by using the Hubbard-Stratanovich transformation. The Ising variable n_i is replaced by the Ising field $\psi(i)$ and the variable σ_i is replaced by the s component field $\phi_i^{(1)}$, $1=1,\ldots,s$.

The mean-field theory is derived by assuming that the Ising field and one of the components of the Potts field orders uniformly in space. The resulting Hamiltonian is

$$F=\tfrac{1}{2}(s-1)r_1\tilde{\phi}^2-(1/3!)w_1(s-1)(s-2)w_1\tilde{\phi}^3 -\tfrac{1}{2}w_2(s-1)\psi\tilde{\phi}^2-\tfrac{1}{2}\epsilon\psi^2+\alpha\psi^4+h\psi-(s-1)H\tilde{\phi}\ , \tag{3.2}$$

where α, ϵ, and h are as defined above. The factors w_1 and w_2 are finite and nonzero, and r_1 is a function of J. The field ψ is the Ising order parameter, while $\tilde{\phi}$ is the percolation order parameter, giving the connectivity properties and exponents. We recover the Ising free energy if we set $s=1$:

$$F=\alpha\psi^4-\epsilon\psi^2+h\psi\ . \tag{3.3}$$

The percolation free energy is given by[36]

$$\left.\frac{dF}{ds}\right|_{s=1}=\tfrac{1}{2}(r_1-w_2\psi)\tilde{\phi}^2+(1/3!)w_1\tilde{\phi}^3-H\tilde{\phi}\ . \tag{3.4}$$

The Ising free energy in Eq. (3.3) is the same as the free-energy density in Eq. (2.3) for a uniform state, and hence it has the spinodal magnetic field $h_{\rm sp}$, and the spinodal value of the order parameter, $\psi_{\rm sp}$, calculated above. From (3.4), the percolation threshold occurs at $r_1=w_2\psi$.[35] We see that the choice $r_1=w_2\psi_{\rm sp}$ makes the mean-field spinodal line coincide with a percolation line.[9,37] With this choice, the free energy in (3.4) is the cubic free-energy density appropriate close to the spinodal; thus the percolation exponents for this percolation model will be the same as the spinodal exponents. The spinodal correlation length ξ will diverge with the same exponent as the percolation connectedness length ξ_p; similarly, the spinodal susceptibility has the same exponent as the percolation mean cluster size.

Since the nucleating droplet has a diameter the same order of magnitude as the spinodal correlation length, we expect these fluctuations to have the same structure as percolation clusters with connected length ξ near the percolation threshold. The fractal dimension[38] d_f of the nucleating droplets at the spinodal is thus the same as the fractal dimension of a percolation cluster, which implies $d_f<d$.

IV. LIFETIME

The main contribution to the partition function for the metastable state comes from integrating in the neighborhood of the metastable minimum; however, the nucleating droplet samples the saddle point separating the two minima. If we include contributions to Z from close to the saddle point as well as from near the metastable minimum, we integrate along one direction in which the integrand increases as we move away from the saddle point, rather than decreases. If we perform a simple Gaussian approximation, this direction would lead to a divergent result. We remove this divergence by an analytic continuation of the Gaussian integral;[5,39] this analytic continuation is implicit in our treatment of the metastable phase as the continuation of the stable phase around 0 magnetic field in the complex plane. Upon removing the spurious divergence by deforming the contour of the integral, we find that the contribution to Z from the region near the saddle point becomes complex. The imaginary part of the metastable free energy, or $\mathrm{Im}(\ln Z)$, is related to the lifetime of the state

$$\tau^{-1}=\lim_{V\to\infty}\left[\frac{\mathrm{Im}(\ln Z)}{V}\right]f_d\ . \tag{4.1}$$

f_d is a dynamic prefactor, which we specify later.

We begin the calculation of τ by writing

$$Z=Z_0+Z_1=Z_0(1+Z_1/Z_0)\ , \tag{4.2}$$

where Z_0 is due to the integrations near the metastable minimum, and Z_1 is due to the integrations near the saddle point. We compute both Z_0 and Z_1 by performing quadratic expansions of $H(u)$ around the respective stationary points of H, and evaluating the resulting Gaussian integrals. For the metastable minimum we find

$$Z_0=e^{-H(u_{\rm ms})}\prod_p\left[\frac{\pi}{\omega_p^{(0)}}\right]^{1/2}\ , \tag{4.3}$$

where the $\omega_p^{(0)}$ are the eigenvalues of the free-particle Schrödinger equation

$$(-\tfrac{1}{2}\nabla^2-\epsilon+6\alpha\sigma_{\rm ms}^2)\nu_p^{(0)}(r)=\omega_p^{(0)}\nu_p^{(0)}(r)\ . \tag{4.4}$$

The saddle point gives similar results,

$$Z_1=e^{-H(u_{\rm saddle})}\prod_q\left[\frac{\pi}{\omega_q}\right]^{1/2}\ , \tag{4.5}$$

where the ω_q are the eigenvalues of Eq. (2.18), which is

equivalent to the above Schrödinger equation with a potential.

Thus, we can write

$$\frac{Z_1}{Z_0}=\exp[H(u_{\rm ms})-H(u_{\rm saddle})] \times\prod_q\left[\frac{\pi}{\omega_q}\right]^{1/2}\Big/\prod_p\left[\frac{\pi}{\omega_p^{(0)}}\right]^{1/2}, \tag{4.6}$$

$$=\exp[H(u_{\rm ms})-H(u_{\rm saddle})] \times\exp\left[\int d\omega\,\tfrac{1}{2}\ln\left[\frac{\pi}{\omega}\right][\rho(\omega)-\rho^0(\omega)]\right], \tag{4.7}$$

where $\rho(\omega)$ is the density of states for Eq. (4.4) and $\rho^0(\omega)$ is the density of states for Eq. (2.18). The attractive potential in Eq. (2.18) creates one bound state and d independent translational modes of that state. Each of these $d+1$ states is discrete and is more easily handled in the form of Eq. (4.6) than with what would be highly singular density functionals in Eq. (4.7).

The negative eigenvalue, found in Eq. (2.19b), can be simply inserted into the square root; this is justified through the analytic continuation argument above. We obtain

$$Z_1\propto i^{\frac{25}{6}}(\Delta\tilde{\lambda})^{1/4}. \tag{4.8}$$

The d translational modes must be handled separately since the integrand does not decay as we move away from the stationary point, and thus we cannot perturb around that point. We can choose

$$\delta v_i=\frac{\partial\bar{v}}{\partial x_i}dx_i,\quad i=1,2,\ldots,d \tag{4.9}$$

for the d orthogonal translational modes. Then we have[5,39]

$$|\delta v_i|=|\delta x_i|\left|\frac{1}{d}\int(\vec{\nabla}\bar{v})^2dr\right|^{1/2}, \tag{4.10}$$

and

$$\int\delta v_1\delta v_2\cdots\delta v_d=\left|\frac{1}{d}\int(\vec{\nabla}\bar{v})^2dr\right|^{d/2}\int d^dr\propto(\Delta\tilde{\lambda})^{3d/8}V. \tag{4.11}$$

We are now left with just the continuum states with $\omega_q>0$, which can be handled by a density functional.[5]

We wish to evaluate

$$I=\int d\omega\ln\left[\frac{\pi}{\omega}\right][\rho^0(\omega)-\rho(\omega)]. \tag{4.12}$$

Near the spinodal we can neglect the effect of the quartic term in the free energy on Eq. (2.12) and (4.4), and hence there is only one parameter that sets the energy scale in both Schrödinger equations, $(\Delta\tilde{\lambda})^{1/2}$. If we rescale the variables $\omega'=\omega/(\Delta\tilde{\lambda})^{1/2}$, then we find, setting $\rho'=(\Delta\tilde{\lambda})^{1/2}\rho$,

$$I=\int_0^\infty d\omega'\ln(\omega')[\rho^{0\prime}(\omega')-\rho'(\omega')] +\ln\left[\frac{(\Delta\tilde{\lambda})^{1/2}}{\pi}\right]\int_0^\infty[\rho^0(\omega)-\rho(\omega)]d\omega \tag{4.13a}$$

$$=C+(1+d)\ln\left[\frac{(\Delta\tilde{\lambda})^{1/2}}{\pi}\right]. \tag{4.13b}$$

The first term in Eq. (4.13a) is a definite integral over a dimensionless variable and must therefore be a constant. The second term is evaluated by noting that the integral runs only over continuum states; for ρ^0, all states are continuum states while for ρ, $1+d$ states are bound. The integral thus evaluates to $1+d$.[5]

The dynamic prefactor f_d depends on whether the order parameter is conserved. In the case of nonconserved order parameter, Langer[40] has shown that the prefactor is

$$f_d=\omega_1/\pi kT. \tag{4.14}$$

Since the lifetime is proportional to $(f_d)^{-1}$, the fact that $f_d\to0$ at the spinodal is equivalent to critical slowing down. The conservation of the order parameter introduces another factor slowing down the nucleation. Since the droplet grows by diffusion, all dynamic equations have an extra ξ^2 factor, and the dynamic prefactor is divided by the correlation-length squared[31]

$$f_d=\omega_1/\pi kT\xi^2. \tag{4.15}$$

Combining these results we obtain

$$\frac{Z_1}{Z_0}=C_1V(\Delta\tilde{\lambda})^{(1/2+5d/8)}e^{-\Delta F}. \tag{4.16}$$

If we assume Z_1/Z_0 is small, we can calculate τ by expanding the ln in Eq. (4.1). We should note, however, that Z_1 is calculated assuming only one nucleating droplet in the entire system. A real system nucleates with many droplets at once; there should be contributions to Z from stationary states with an arbitrary number of independent separated droplets. Only if we write

$$Z=Z_0[1+Z_1/Z_0+\tfrac{1}{2}(Z_1/Z_0)^2+\cdots] \cong Z_0e^{(Z_1/Z_0)}, \tag{4.17}$$

will the free energy be an extensive quantity, increasing linearly with the system's volume V.[5] Upon using Eq. (4.16) and (4.17) in (4.1), we find the lifetime

$$\tau\sim(\Delta\tilde{\lambda})^{-[1+(5/8)d]}\exp\left[k\frac{\epsilon^{2-d/2}}{2\alpha}(\Delta\tilde{\lambda})^{3/2-d/4}\right]. \tag{4.18}$$

V. DISCUSSION

We have extended Langer's work on nucleation near $h=0$ to magnetic fields near the spinodal $h=h_s$ for long-range potentials. In Langer's treatment, which assumes compact droplets, the infinite-range interaction limit gives trivial results. As the range of the interaction increases, so does the free-energy cost of the nucleating droplets, and the nucleation rate goes to 0. For a large magnetic field the droplets can have a radius proportional to R, and not

have a large free-energy cost. Thus, for $h>0$ and $R\to\infty$, the droplets are ramified and produce nontrivial mean-field results. For nonzero magnetic fields the noncompact droplets, having a positive "surface" energy and a negative bulk magnetic energy both proportional to the number of spins in the droplet, can enter with nonzero weight, even in the limit of large radii. The greatly increased entropy of these ramified fluctuations enters into their free-energy cost, which in this case is not simply approximated by the energy cost as it was near $h=0$. Thus, while the nucleation rate goes to 0 as $R\to\infty$ for $h<h_s$, h_s is independent of R, and for $h=h_s$ we still see the spinodal instability. Thus, while the weak singularity[5] at $h=0$ disappears in the limit $R\to\infty$, the spinodal singularity becomes well defined.

For fixed R, our results cross over to those of Langer[5] as h is varied from h_s to 0. This crossover has been studied in three dimensions by Cahn and Hilliard,[3] who found the profile of the nucleating droplet for intermediate values of the magnetic field. The profile changes continuously between the hyperbolic tangent solution near $h=0$ to the small-amplitude diffuse solution of Eq. (2.10) near the spinodal.[25] They found spinodal exponents that are twice ours, which is the expected relation between exponents for order parameter versus conjugate field quenches.

Consistent with Cahn and Hilliard we find for $d<6$ that the free-energy cost of the nucleating droplet goes to 0. This result contrasts with that of Sarkies and Frankel,[14] who find that the free-energy cost in three dimensions remains constant at the spinodal. We find a constant free energy only for six dimensions. We find, for the nucleating droplet, the scaling results

$$\xi\sim R(h_s-h)^{-1/4},\quad \nu=\tfrac{1}{4} \tag{5.1a}$$

$$(\Delta\nu)_{\text{droplet}}\propto(h_s-h)^{1/2},\quad \beta=\tfrac{1}{2} \tag{5.1b}$$

and obtain nonclassical ramified droplets with mean-field exponents.

Although Cahn and Hilliard studied the nucleating droplet profile, they did not treat the initial growth mode. Our calculation of an initial growth mode which is centered at the origin is in contrast to Langer's calculation for $h=0$. For small fields the growth mode is peaked at the surface of the droplet, corresponding to growth occurring through increasing radius, with the concentration at the center of the droplet remaining fixed at the stable magnetization. Near the spinodal the growth mode is peaked at the origin, implying that the growth occurs by spins filling in the center of the droplet; the average radius of the droplet initially decreases. This is consistent with computer experiments on the three-dimensional Ising model.[9,10] These computer experiments were done using Glauber dynamics with no conserved order parameter; computer studies of the initial growth mode for conserved dynamics would be of considerable interest. While the nucleating droplet is independent of the dynamics,[3] the initial growth mode may depend on the dynamics.

The lifetime of the metastable state depends both on the nucleating droplet and on the droplet's growth modes; it includes the free-energy cost of the droplet as an exponential factor, while the prefactor of the exponential depends on the growth modes of the droplet. The dynamical prefactor to the lifetime diverges as the spinodal is approached; thus there is critical slowing down at the spinodal line in all dimensions.[26]

We have shown that the upper critical dimension for quenches to the spinodal away from the critical point is 6, and that if we quench toward the critical point along the coexistence curve, the upper critical dimension is 4, in agreement with Binder.[33] Somewhat more surprising is the fact that, for our field-theoretic model, the upper critical dimension varies smoothly from 4 to 6, depending on the path of the quench. This conclusion requires that we be able to calculate $h_s(T)$ exactly in order to be able to define the parameter $[h_s(T)-h]/h_s(T)$ along the quench in the h,T plane. Within our model, $h_s(T)$ is determined precisely by the constants ϵ and α. In other models, such as the Ising model, or in experimental systems, the mean-field line becomes an extended spinodal region; there are no precise values for ϵ, α, or the spinodal field in these systems.[21] Thus whenever the spinodal region is diffuse, we do not expect a continuously changing upper critical dimension as we cross over from spinodal to critical behavior. For the two types of limiting quenches, quenching to the critical point along the coexistence curve and quenching straight to the spinodal line staying away from the critical point, the exact location of the spinodal line or region is irrelevant; thus the lack of definition in the spinodal region does not affect the upper critical dimension for those two types of quenches.

We are presently extending this work in two directions. First we are studying in more detail the crossover between the behavior at small magnetic field and the behavior at fields near the spinodal. We are also extending our treatment of the dynamics of the growth of the nucleated droplet.

Note added in proof. After submission of this paper, it has come to our attention that the results in Eqs. (2.10) and (2.19) have been derived by M. Büttiker and R. Landauer [Phys. Rev. A 23, 1397 (1981)].

ACKNOWLEDGMENTS

We are pleased to acknowledge useful and stimulating discussions with K. Binder, E. T. Gawlinski, D. W. Heermann, A. Sawyer, and D. Stauffer. We would especially like to thank J. D. Gunton for valuable conversations throughout this work. One of us (C.U.) gratefully acknowledges the support of a National Science Foundation (NSF) fellowship. We would like to acknowledge additional support from the NSF in the form of Materials Research Program Grant No. DMR-82-15648. The center for Polymer Studies is partially supported by grants from U.S. Army Research Office, National Science Foundation, and U.S. Office of Naval Research.

APPENDIX

In this Appendix we show that the equation

$$-\frac{d^2x}{dt^2}-\frac{2}{t}\frac{dx}{dt}+\frac{4}{3\sqrt{3}}-\frac{6}{\sqrt{3}}x^2=0\,, \tag{A1}$$

has a solution with the boundary conditions

$$\left.\frac{dx}{dt}\right|_{t=0}=0 \tag{A2a}$$

and

$$x(t=\infty)=\sqrt{2}/3\ . \tag{A2b}$$

We have renamed variables, $x=v$ and $t=-s$, from Eq. (2.8) so that the mechanical analogy is more apparent. This equation is the equation of motion for a particle with unit mass, with damping inversely proportional to time, and potential energy pictured in Fig. 6. The boundary conditions are that the particle is released from rest on the slope to the left, and comes to rest exactly at x_p. It is obvious that a particle released near the bottom of the small well will eventually come to rest at the bottom of that well, due to the damping. We only need to show that as the particle is released from positions higher up along the slope to the left it will, for some initial height, have sufficient energy to travel over the barrier hill. From continuity, there must be a height separating the two extremes where the particle passes over the barrier and where it becomes trapped in the potential well centered at $-\sqrt{2}/3$. This height is the initial height of the solution we are interested in.

We can show that there must be a path that passes over the barrier by bounding the dissipation term. After letting the particle travel for time t_0 we replace the time-dependent damping coefficient by the constant $2/t_0$, which is greater than $2/t$ for all further times. If the particle has sufficient energy to pass over the barrier with damping constant $2/t_0$, it would certainly pass over the barrier with the time-dependent damping.

The particle feels a force of $4/\sqrt{3}$ at the point a in Fig. 6. It feels a larger force at the points it reaches before point a. Thus by starting the particle sufficiently far to the left, we can make its velocity at a as close as we like to the terminal velocity for a force of $4/\sqrt{3}$ and a damping constant $2/t_0$, i.e., $\mathscr{V}_t=2t_0/\sqrt{3}$. We take the velocity at point a to be $\mathscr{V}_a=2ft_0/\sqrt{3}$, where f is smaller than but arbitrarily close to one; the velocity must be at least this large, and if it is larger the particle would be even more likely to go over the barrier.

The velocity at the bottom of the well is then at most

$$\mathscr{V}_{\max}=\left[\mathscr{V}_a^2+\frac{32\sqrt{6}}{9}\right]^{1/2},$$

which can be found by ignoring the damping. The largest damping term at any point on the path is less than

$$\frac{2}{t_0}\mathscr{V}_{\max}=\left[\tfrac{16}{3}f^2+\frac{8\sqrt{6}}{9t_0^2}\right]^{1/2}\equiv\gamma \tag{A3}$$

Setting this into Eq. (A1) will cause the particle to come to rest earlier.

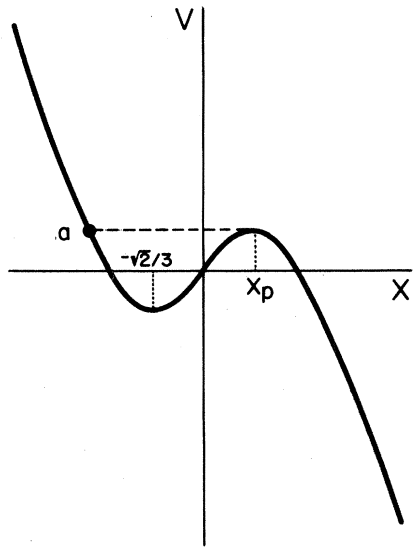

FIG. 6. Sketch of the potential in Eq. (A1).

We are left with the question of whether a particle obeying

$$-\frac{d^2x}{dt^2}+\gamma+\frac{4}{3\sqrt{3}}-\frac{6}{\sqrt{3}}x^2=0\ , \tag{A4}$$

and starting at point a, $x=-2\sqrt{2}/3$, with velocity $\mathscr{V}_a=f(2t_0/\sqrt{3})$ will travel farther than the peak of the original barrier, $x_p=\sqrt{2}/3$. It is easy to integrate Eq. (A4) to find

$$\left[\frac{dx}{dt}\right]^2=\tfrac{4}{3}f^2t_0^2+\left[\gamma+\frac{4}{3\sqrt{3}}\right]\left[x-\frac{\sqrt{2}}{3}\right]-\frac{2}{\sqrt{3}}\left[x^3-\frac{2\sqrt{2}}{27}\right]. \tag{A5}$$

As t_0 is increased, all terms on the right-hand side of the equation except the first remain bounded. For sufficiently large t_0 there can be no cancellation of the first term for $|x|<\sqrt{2}/3$ and hence this particle goes over the barrier. Thus if we can take t_0 sufficiently large, the original particle passes over its barrier. We can take t_0 to be as large as we like by starting the particle far to the left; the particle cannot travel an indefinitely large distance in the definite time t_0 without having an unboundedly large velocity.

Since there exists at least one solution where the particle clears the barrier, as we increase the height from which the particle is started in Fig. 6 there must come a starting height where the particle first makes it over the barrier. This height, which divides the starting heights for bounded and unbounded solutions, must be the initial height for a solution that comes to rest on top of the barrier.

[1]*Nucleation*, edited by A. C. Zettelmoyer (Dekker, New York, 1969); F. F. Abraham, *Homogeneous Nucleation Theory* (Academic, New York, 1974).
[2]J. W. Cahn, Trans. Metal. Soc. AIME 242, 166 (1968).
[3]J. W. Cahn and J. E. Hilliard, J. Chem. Phys. 28, 258 (1958); 31, 688 (1959).
[4]J. L. Lebowitz and O. Penrose, J. Math. Phys. 7, 98 (1967).
[5]J. S. Langer, Ann. Phys. (N.Y.) 41, 108 (1967).
[6]O. Penrose and J. L. Lebowitz, in *Studies in Statistical Mechanics*, edited by E. W. Montroll and J. L. Lebowitz (North-

Holland, Amsterdam, 1978), Vol. 7.
[7]C. Domb and H. W. Dalton, Proc. Phys. Soc. London 89, 859 (1966).
[8]D. W. Heermann, W. Klein, and D. Stauffer, Phys. Rev. Lett. 49, 1262 (1982).
[9]D. W. Heermann and W. Klein, Phys. Rev. B 27, 1732 (1983).
[10]D. W. Heermann and W. Klein, Phys. Rev. Lett. 50, 1062 (1983).
[11]D. Stauffer, A. Coniglio, and D. W. Heermann, Phys. Rev. Lett. 49, 1299 (1982).
[12]J. D. Gunton, M. San Miguel, and P. S. Sahni, in *Phase Transitions and Critical Phenomena,* edited by C. Domb and J. L. Lebowitz (Academic, New York, 1983), Vol. 8.
[13]W. Klein, Phys. Rev. Lett. 47, 1569 (1981).
[14]K. W. Sarkies and N. E. Frankel, Phys. Rev. A 11, 1724 (1975).
[15]W. Klein and C. Unger, Phys. Rev. B 28, 445 (1983).
[16]K. Binder and D. Stauffer, Phys. Rev. Lett. 33, 1006 (1974).
[17]C. Billotet and K. Binder, Z. Phyz. B 32, 195 (1979).
[18]B. Chu, F. J. Schoenes, and M. E. Fisher, Phys. Rev. 185, 185 (1969).
[19]R. J. Speedy and C. A. Angell, J. Chem. Phys. 65, 851 (1976).
[20]T. Kawasaki, T. Imaeda, and J. D. Gunton, in *Perspectives in Statistical Physics, M. S. Green Memorial Volume,* edited by H. J. Ravache (North-Holland, Amsterdam, 1981).
[21]K. Kaski, K. Binder, and J. D. Gunton, J. Phys. A 16, L623 (1983).
[22]K. Binder, C. Billotet, and P. Mirold, Z. Phys. B 30, 183 (1978).
[23]J. S. Langer, Physica (Utrecht) 73, 61 (1974).
[24]J. D. Gunton and M. C. Yalabik, Phys. Rev. B 18, 6199 (1978).
[25]C. Unger, thesis, Boston University (unpublished, 1984).
[26]K. Binder, Phys. Rev. B 8, 3423 (1973).
[27]A. J. Schwartz, S. Krishnamurthy, and W. I. Goldburg, Phys. Rev. A 21, 1331 (1980); S. Krishnamurthy and W. I. Goldburg, *ibid.* 22, 2147 (1980).
[28]R. B. Heady and J. W. Cahn, J. Chem. Phys. 58, 896 (1973).
[29]J. S. Huang, W. I. Goldburg, and M. R. Moldover, Phys. Rev. Lett. 34, 639 (1975).
[30]R. G. Howland, N. C. Wong, and C. M. Knobler, J. Chem. Phys. 73, 522 (1980).
[31]J. S. Langer and A. J. Schwartz, Phys. Rev. A 21, 948 (1980).
[32]K. Binder and D. Stauffer, Adv. Phys. 25, 343 (1976).
[33]K. Binder, Phys. Rev. A 29, 341 (1984).
[34]A. Coniglio and W. Klein, J. Phys. A 13, 2775 (1980).
[35]A. Coniglio and T. C. Lubensky, J. Phys. A 13, 1783 (1980).
[36]P. W. Kastaleyn and C. M. Fortuin, J. Phys. Soc. Jpn. (Suppl.) 26, 11 (1969).
[37]D. W. Heermann, A. Coniglio, W. Klein, and D. Stauffer (unpublished).
[38]B. Mandelbrot, *The Fractal Geometry of Nature* (Freeman, San Francisco, 1982).
[39]L. Shulman, *Techniques and Applications of Path Integration* (Wiley, New York, 1981).
[40]J. S. Langer, Ann. Phys. (N.Y.) 54, 158 (1969).